Proceedings Paper:
Kennedy, C.D., Reaney, I.M. orcid.org/0000-0003-3893-6544 and Dean, J.S. orcid.org/0000-0001-7234-1822 (2018) Finite element study of the effect of particle interaction on the energy storage density of composite dielectrics. In: Energy Procedia. 3rd Annual Conference in Energy Storage and Its Applications, 11-12 Sep 2018, Sheffield, UK. Elsevier , pp. 129-134.

https://doi.org/10.1016/j.egypro.2018.09.037

Available online at www.sciencedirect.com

ScienceDirect

Energy Procedia 151 (2018) 129–134

Energy Procedia

www.elsevier.com/locate/procedia

3rd Annual Conference in Energy Storage and Its Applications, 3rd CDT-ESA-AC, 11–12 September 2018, Sheffield, UK

Finite element study of the effect of particle interaction on the energy storage density of composite dielectrics.

Carl D. Kennedy, Ian M. Reaney, Julian S. Dean.

The University of Sheffield, Sheffield S10 2TN, United Kingdom

Abstract

Finite element methods can be used to study the effect of microstructure on the electrical properties of dielectric materials. These tools are utilized here to study particle interaction in composite dielectrics. The orientation and alignment of particles with each other and the applied potential difference are shown to have varying effects on the electrical breakdown strength of the composite and consequently the energy storage density. Due to an increased electrical field magnitude in the polymer matrix between particles. This increased electric field may initiate electrical breakdown in the polymer at a lower applied potential difference than would be expected for the pure polymer adversely affecting the energy storage density of dielectric composites.

Keywords: breakdown strength; composite; dielecric; energy storage density; finite element method;

1. Introduction

With the increased demand for technologies such as electric vehicles, there is a need to develop high energy density dielectrics for capacitors which can deliver high power for a short period of time [1-3]. The maximum energy storage density, U_{max}, of dielectrics can be calculated using $U_{max} = 1/2\ \varepsilon_0 \varepsilon_r E_{bd}^2$ where ε_0 is the permittivity of free space, ε_r and E_{bd} are the relative permittivity and electrical breakdown strength of the dielectric, respectively. A common way to develop these dielectric materials is by introducing high permittivity particles, such as $BaTiO_3$, into a high breakdown strength polymer [4-6]. One such polymer is polymethylmethacrylate (PMMA) with $\varepsilon_r = 3$ and $E_{bd} = 8\ MV.cm^{-1}$ [7], above this threshold field the dielectric is statistically likely to lose its insulating ability and incur irreversible damage. Due to its moderate intrinsic permittivity (ε_r = 62) and room temperature fabrication [8], methylammonium lead iodide (MALI) ($E_{bd} = 20\ kV.cm^{-1}$ [9]) is a promising candidate as a distributed particulate in polymer composites.

10.1016/j.egypro.2018.09.037

Nomenclature

ε_r	relative permittivity	PMMA	polymethylmethacrylate
E_{bd}	electrical breakdown strength	MALI	methylammonium lead iodide
$\boldsymbol{E_n}$	normalised electric field	FEM	finite element methods

However, the introduction of particles into the polymer matrix usually causes the breakdown strength of the composite to be reduced relative to that of the pure polymer [2, 10]. As the maximum energy storage density is quadratically dependent on E_{bd} it is important to understand how particle interaction acts to reduce E_{bd}. Hence informing better design strategies for composite dielectrics. To study the effect of particle interaction on the E_{bd} of PMMA / MALI composite dielectrics finite element methods (FEM) are utilised.

The effect of microstructural changes on the electric field and permittivity in functional oxides and composite materials have previously been studied using FEM [10-16]. A finite element package has been developed in-house, which for a known geometry solves Maxwell's equations in 3D space and time [13-15]. To better represent the geometry of composites, a full 3D is required, as it results in a more accurate prediction of the electrical response compared to two-dimensional simulations [17, 18]. In this work simple two-particle MALI / PMMA composites are simulated to study the effect of interacting particles and provide design criteria for increased performance.

2. Particle interaction response

To study the effect of the relative orientation of particles within the polymer, we generate a simple model containing two particles with radius 10 µm surrounded by a polymer matrix, a cube with side length of 100 µm, as shown in Fig. 1(a). The particles are aligned with their centres either parallel (Fig. 1b) or perpendicular (Fig. 1b (inset)) to the applied potential difference of 1V. The distance between the particles is then varied from the centre of the cube, as depicted in Fig. 1 (b).

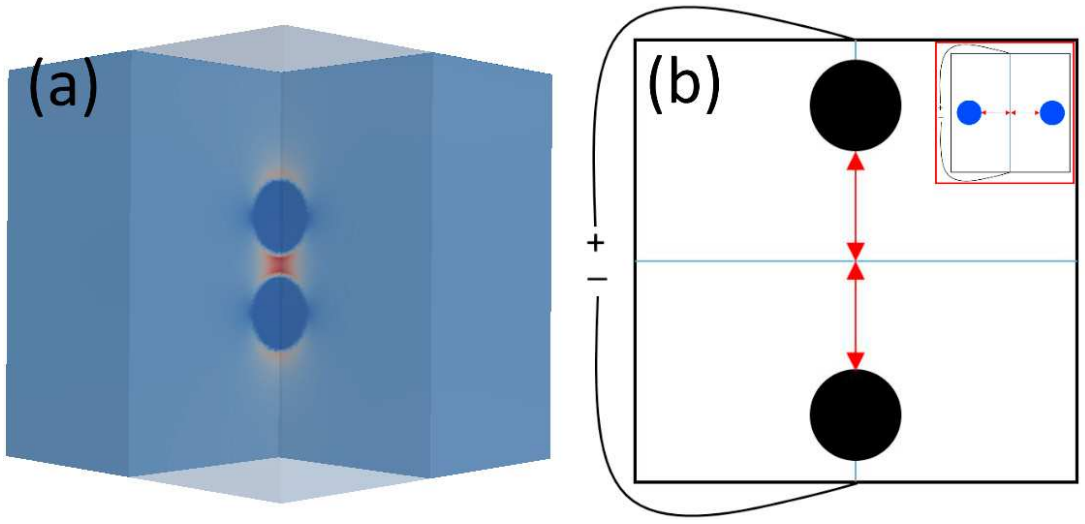

Fig. 1 (a) showing 3D geometry and electric field plot of two particles in a cube (side=100μm), red and blue indicating high and low electric fields respectively. (b) illustration of a 2D slice through the centre of two particles equidistant from the centre of the cube. Shown are particles parallel and perpendicular (inset) to the applied electric field. Double headed arrow showing distances of equal length. Blue lines intersect the cube into quadrants.

The models are then meshed with tetrahedra using the software GMSH [19] with a finer mesh size produced around the particles to account for the complexity of the electric field at that point. A convergence test was then performed to

find the most suitable mesh size to ensure confidence in the solution as well as to reduce simulation time, resulting in models possessing approximately 40k elements.

Each material volume is then assigned its own value of conductivity σ and permittivity ε_r. The material properties of MALI ($\varepsilon_r = 62$, $\sigma = 3\text{x}10^{-7}$ S.cm^{-1}) and PMMA ($\varepsilon_r = 3.07$, $\sigma = 1\text{x}10^{-16}$ S.cm^{-1}) were then assigned to each of the desired regions [20]. This was then solved using ELCer to extract the effective capacitance and hence permittivity of the system since $C = \varepsilon_0 \varepsilon_r A/d$ where A and d are the cross-sectional area and thickness of the dielectric material, respectively. More details of this approach can be found in [13]. Verification of the model was carried out by simulating both pure MALI and PMMA with the resulting effective permittivity and conductivity agreeing with the input parameters. For a comparison, a cube of pure PMMA generates a uniform electric field of 100 MVm^{-1} with the application of 1 V of potential difference across the contacts. This is then used to normalise the electric field ($\mathbf{E}_n$) of the resulting simulations in order to highlight the increase in electric field due to the interacting particles of MALI.

We first look at the orientation of the MALI particles perpendicular to the applied field. Fig. 2 (a)-(d) show a plane cut through the centre of two MALI particles inside the PMMA, with separations of 1, 5, 10 and 15 µm respectively. A stream line analysis is overlaid on the geometrical outline of the model, highlighting the vector path of the electric field. As MALI is more conducting it behaves conversely from a pore or void. This means that instead of the current flowing around it, the current wants to flow through this least resistive region. As such there is a constriction above and below the particles. This generates an increased electric field in the PMMA close to the surface of the particles of approximately 2.4 times when compared to the system with no particles present. In Fig. 2 (a) and (e) two particles are not interacting and two separate responses can be seen along the central 'x' axis. As the two particles are moved closer together we can see they act to reduce the field between them, essentially behaving like a single particle when the separation is less than 1 µm.

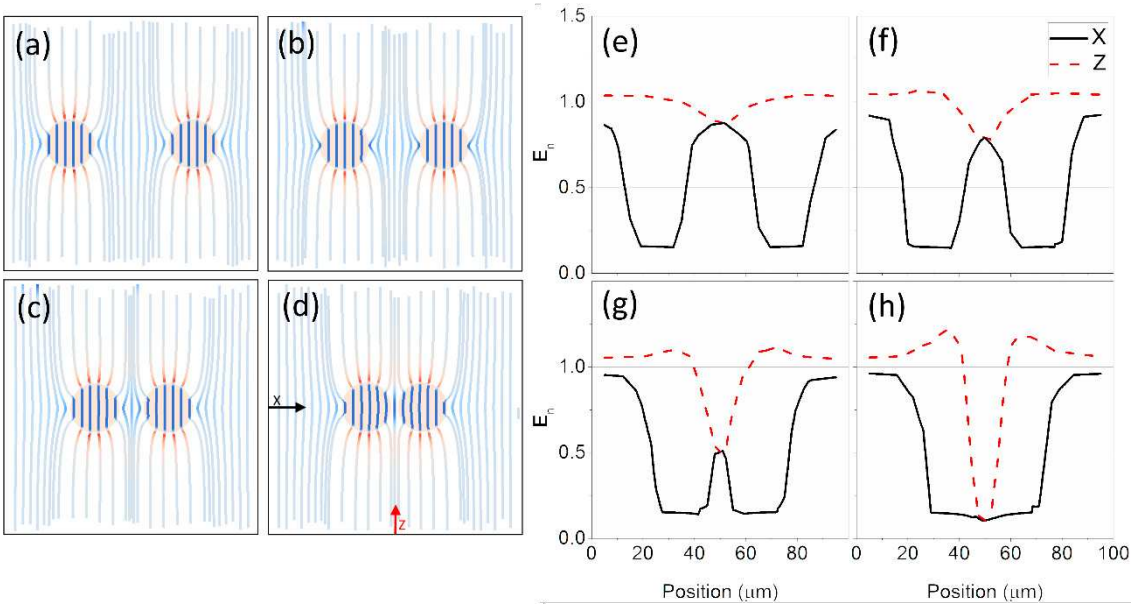

Fig. 2 The effect of separation on $\mathbf{E}_n$ for two particles aligned perpendicular to the electric field applied across top to bottom. 2D slices showing electric field strengths through the centre of the particles. The colour maps from weakest (blue) to strongest (red) electric field. The profiles are for particles with radius 5 µm, with separations of 1 (a), 5 (b), 10 (c) and 15 µm (d). (e)-(h) show the fields corresponding to the respective profiles in (a)-(d) along both the central x-axis and z-axis (black and red arrows, respectively, shown in (a), parallel and perpendicular, respectively, to the applied field.

Similarly, we look at the case of the two MALI particles aligned parallel to the applied field, Fig. 3 (a) – (d). However, in this case as the two particles are brought closer together the electric field in-between is concentrated, and as their

separation approaches the diameter of the particles (Fig. 3) the electric field in between the particles increases to near twice that of the pure PMMA. At 1µm apart (Fig. 3), it can be seen that the electric field is now over 3.3 times that of the PMMA.

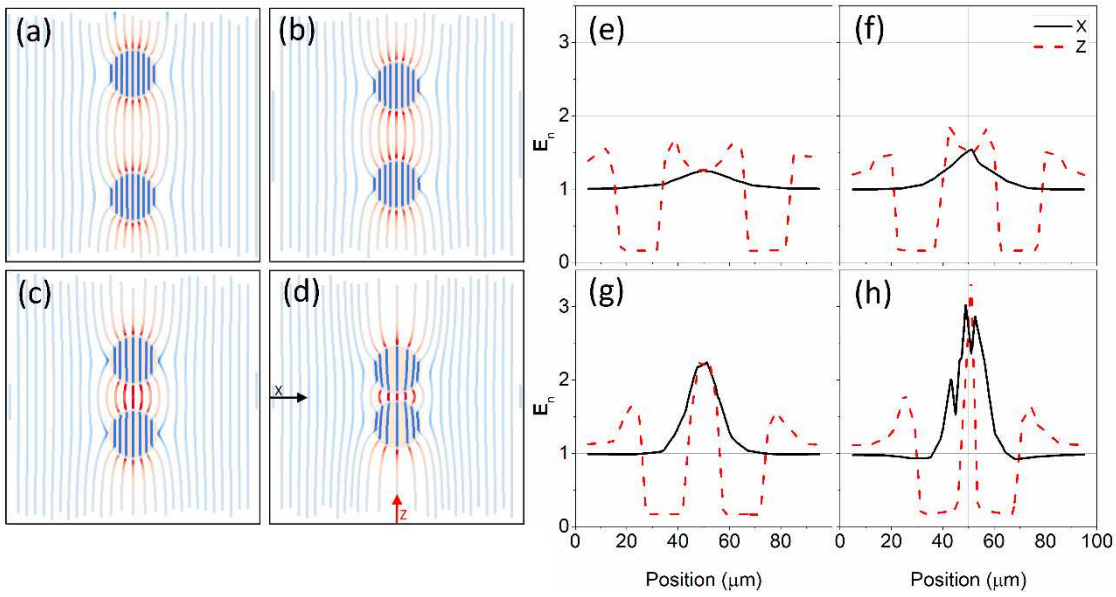

Fig. 3 The effect of separation on $\mathbf{E}_n$ for two particles aligned parallel to the electric field applied across top to bottom. 2D slices showing electric field strengths through the centre of the particles. The colour maps from weakest (blue) to strongest (red) electric field. The profiles are for particles with radius 5 µm, with separations of 15 (a), 10 (b), 5 (c) and 1 µm (d). (e)-(h) show the fields corresponding to the respective profiles in (a)-(d) along both the central x-axis and z-axis (black and red arrows, respectively, shown in (a), parallel and perpendicular, respectively, to the applied field

Thus, the orientation of particles relative to one another has an important effect, either intensifying (parallel particle alignment) or reducing (perpendicular particle alignment) the electric field in the polymer matrix between particles. It is therefore probable that the polymer matrix breakdown strength is the determining factor when calculating the E_{bd} of the composites. Fig. 4 shows the E_{bd} of the composites relative to that of the pure polymer for various geometrical configurations of two MALI particles in PMMA. It is assumed that an increase in maximum electric field within the polymer matrix will initiate breakdown so that the breakdown strength of the composite is inversely proportional to the normalised maximum electric field magnitude. In the case of parallel alignment as the separation of particles decreases their interaction increases leading to much higher electric fields, having the effect of reducing the breakdown strength of the composite by more than 90% at 1 µm separation, see Fig. 4.

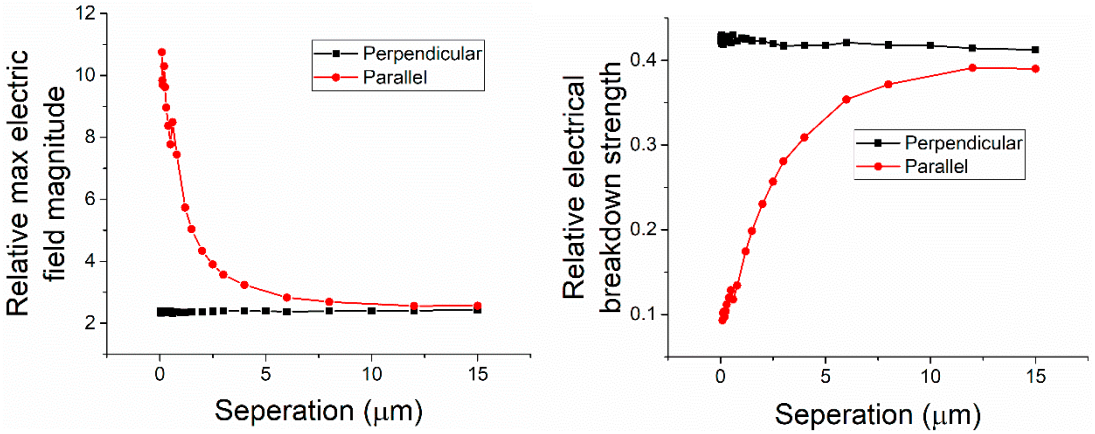

Fig. 4 shows the effect of particle separation, for both perpendicular and parallel cases, on the simulated maximum electric field magnitude and consequently E_{bd} of PMMA/MALI composites.

Particle interaction effects on the E_{bd} of composites have been studied using FEM and showed an increased electric field in the polymer matrix at the upper and lower surfaces of the particles. Consequently, the largest increase of the field was found between closer particles orientated parallel to the applied field. This suggests a way to guide the design of high energy density composite dielectrics. For example, it may be possible to increase breakdown strength by layering one particle thick layers with polymer only layers. It is also obvious that a uniform distribution of particles would lead to a better E_{bd}, highlighting the importance of a good dispersion of particles within the polymer matrix if high energy densities are to be achieved.

Acknowledgements

The authors gratefully acknowledge support from the EPSRC via grant EP/L016818/1 which funds the Centre for Doctoral Training in Energy Storage and its Applications.

References

1. Barber, P., et al., *Polymer Composite and Nanocomposite Dielectric Materials for Pulse Power Energy Storage.* Materials, 2009. **2**(4): p. 1697-1733.
2. Thakur, V.K. and R.K. Gupta, *Recent Progress on Ferroelectric Polymer-Based Nanocomposites for High Energy Density Capacitors: Synthesis, Dielectric Properties, and Future Aspects.* Chemical reviews, 2016. **116**(7): p. 4260-4317.
3. Dang, Z.M., et al., *Fundamentals, processes and applications of high-permittivity polymer matrix composites.* Progress in Materials Science, 2012. **57**(4): p. 660-723.
4. Hoshina, T., *Size effect of barium titanate: fine particles and ceramics.* Journal of the Ceramic Society of Japan, 2013. **121**(1410): p. 156-161.
5. Schumacher, B., et al., *Temperature treatment of nano-scaled barium titanate filler to improve the dielectric properties of high-k polymer based composites.* Microelectronic Engineering, 2010. **87**(10): p. 1978-1983.
6. Padalia, D., et al., *Fabrication and characterization of cerium doped barium titanate/PMMA nanocomposites.* Solid State Sciences, 2013. **19**(Supplement C): p. 122-129.
7. Grabowski, C.A., et al., *Dielectric Breakdown in Silica-Amorphous Polymer Nanocomposite Films: The Role of the Polymer Matrix.* Acs Applied Materials & Interfaces, 2013. **5**(12): p. 5486-5492.
8. Prochowicz, D., et al., *Mechanosynthesis of the hybrid perovskite CH3NH3PbI3: characterization and the corresponding solar cell efficiency.* J. Mater. Chem. A, 2015. **3**(41): p. 20772-20777.
9. Horváth, E., et al., *Nanowires of Methylammonium Lead Iodide (CH3NH3PbI3) Prepared by Low Temperature Solution-Mediated Crystallization.* Nano Letters, 2014. **14**(12): p. 6761-6766.
10. Wang, Z.P., et al., *Dielectric constant and breakdown strength of polymer composites with high aspect ratio*

fillers studied by finite element models. Composites Science and Technology, 2013. **76**: p. 29-36.
11. Myroshnychenko, V. and C. Brosseau, *Finite-element modeling method for the prediction of the complex effective permittivity of two-phase random statistically isotropic heterostructures.* Journal of Applied Physics, 2005. **97**(4).
12. Myroshnychenko, V. and C. Brosseau, *Finite-element method for calculation of the effective permittivity of random inhomogeneous media.* Physical Review E, 2005. **71**(1).
13. Dean, J.S., J.H. Harding, and D.C. Sinclair, *Simulation of Impedance Spectra for a Full Three‐Dimensional Ceramic Microstructure Using a Finite Element Model.* Journal of the American Ceramic Society, 2014. **97**(3): p. 885-891.
14. Heath, J.P., et al., *Simulation of Impedance Spectra for Core–Shell Grain Structures Using Finite Element Modeling.* Journal of the American Ceramic Society, 2015. **98**(6): p. 1925-1931.
15. Dean, J.S., et al., *A resource efficient design strategy to optimise the temperature coefficient of capacitance of BaTiO3-based ceramics using finite element modelling.* Journal of Materials Chemistry A, 2016.
16. Zhao, X., et al., *Three-dimensional simulations of the complex dielectric properties of random composites by finite element method.* Journal of Applied Physics, 2004. **95**(12): p. 8110-8117.
17. Kim, P., et al., *High Energy Density Nanocomposites Based on Surface-Modified BaTiO3 and a Ferroelectric Polymer.* Acs Nano, 2009. **3**(9): p. 2581-2592.
18. Wang, Y., et al., *Filler orientation effect on relative permittivity of dielectric elastomer nanocomposites filled with carbon nanotubes.* Computational Materials Science, 2015. **104**: p. 69-75.
19. Geuzaine, C. and J.-F. Remacle, *Gmsh: A 3-D finite element mesh generator with built-in pre- and post-processing facilities.* International Journal for Numerical Methods in Engineering, 2009. **79**(11): p. 1309-1331.
20. Zheng, W. and S.-C. Wong, *Electrical conductivity and dielectric properties of PMMA/expanded graphite composites.* Composites Science and Technology, 2003. **63**(2): p. 225-235.